Perceiving the Emergence of Hadron Mass through **AMBER@CERN**

10 – 13 May 2022
CERN, Geneve - Switzerland

https://indico.cern.ch/event/1145356/

NRQCD analysis of fixed-target charmonium production and pion PDFs

Wen-Chen Chang

Institute of Physics, Academia Sinica, Taiwan

In collaboration with
Claude Bourrely, Jen-Chieh Peng, Stephane Platchkov, Takahiro Sawada, Chia-Yu Hsieh and Yu-Shiang Lian

Experimental Approaches of Accessing Pion PDFs

- Drell-Yan: $\pi^{\pm}p \to \mu^{+}\mu^{-}X$ (LO: sensitive to valence quarks)
  - **LO: $q\bar{q} \to \mu^{+}\mu^{-}$**
  - NLO: $q\bar{q} \to \mu^{+}\mu^{-}G, qG \to \mu^{+}\mu^{-}q$ (large p_T)
  - NNLO: $q\bar{q}G \to \mu^{+}\mu^{-}G, qG \to \mu^{+}\mu^{-}qG, GG \to \mu^{+}\mu^{-}q\bar{q}$
- Direct photon: $\pi^{\pm}p \to \gamma X$ (LO: sensitive to gluons)
  - **LO: $q\bar{q} \to \gamma G, qG \to \gamma q$**
- Jpsi: $\pi^{\pm}p \to J/\psi X$ (LO: sensitive to gluons)
  - **LO: $q\bar{q} \to c\bar{c} \to J/\psi X, GG \to c\bar{c} \to J/\psi X$**
  - NLO: $q\bar{q} \to c\bar{c}G \to J/\psi X, GG \to c\bar{c}G \to J/\psi X, qG \to c\bar{c}q \to J/\psi X$
- Leading neutron (LN) electroproduction: Sullivan processes from a nucleon's pion cloud

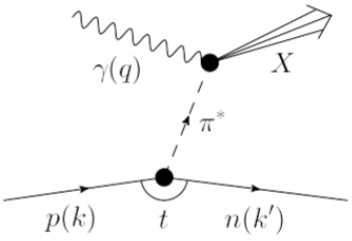

Pion PDFs (2022)

PDF	DY (xF, pT)	Direct γ	J/ψ	LN	Refs.
OW	*		*		PRD 1984
ABFKW	*	*			PLB 1989
SMRS	*	*			PRD 1992
GRV	*	*			ZPC 1992
GRS	*				EPJC 1999
JAM	*			*	PRL 2018 PRD 2021 PRL 2021
xFitter	*	*			PRD 2020
BS, BBP	*		(*)		NPA 2019 PLB 2021 PRD 2022

JAM21: finite qT
[Cao et al., PRD 103, 114014 (2021)]

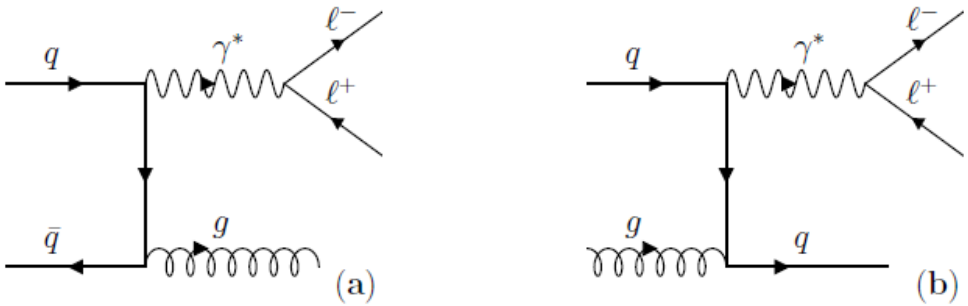

FIG. 1. Examples of LO diagrams for the large transverse momentum region in Drell-Yan lepton-pair production for the $q\bar{q}$ channel (a) and qg channel (b).

$H_{a,b}^{\mathrm{DY}}$ starts at $\mathcal{O}(\alpha_s^0)$, and in our analysis we compute corrections up to $\mathcal{O}(\alpha_s)$. Our study is the first attempt to include both p_{T}-differential and p_{T}-integrated pion-nucleus Drell-Yan data [4, 5] on the same footing, taking advantage of the fact that the p_{T}-dependent cross sections provide access to a larger region of parton momentum fractions relative to the p_{T}-integrated case.

GRV vs. JAM21

GRV

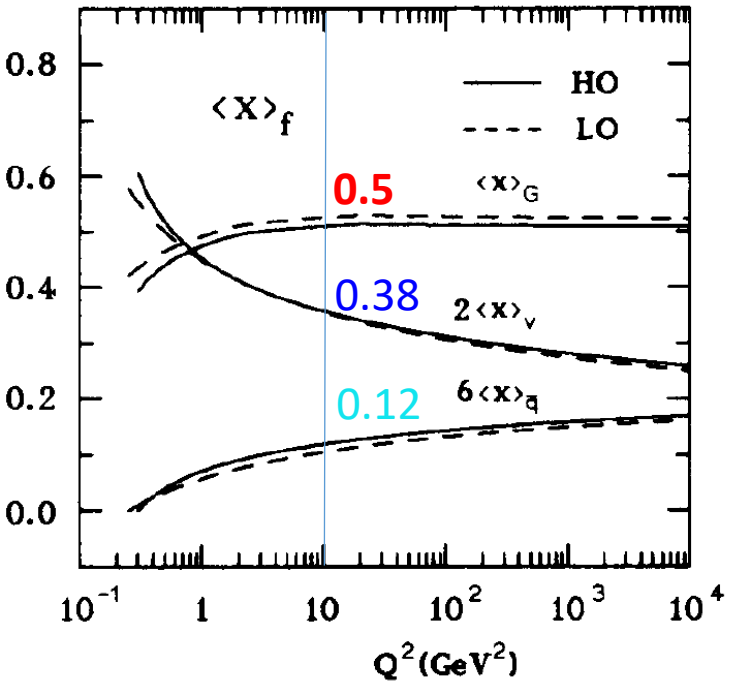

JAM21

	$\mu^2 = 10$ GeV^2		
data sets	$\langle x\rangle_v^\pi$	$\langle x\rangle_s^\pi$	$\langle x\rangle_g^\pi$
DY	0.49(1)	0.26(8)	0.25(8)
DY+LN	0.43(2)	0.17(3)	0.40(4)
DY+LN+DYp_T	**0.44(1)**	**0.19(2)**	**0.37(3)**

The hierarchy of <x> of valence quark and gluon are opposite in GRV and JAM.

JAM21: Threshold Resummation
[Barry et al., PRL 127, 232001 (2021)]

$$(1-x)^{\beta_v^{eff}}$$

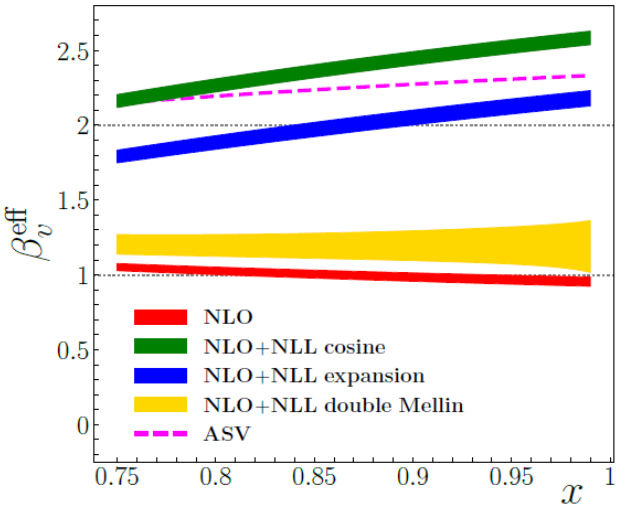

FIG. 3. Effective exponents $\beta_v^{\rm eff}$ for the various prescriptions versus x at the scale μ_0, compared with the ASV extraction [33]. The values $\beta_v^{\rm eff} = 1$ and 2 are shown for reference.

results in a wide variety of $\beta_v^{\rm eff}$ values, with the cosine and expansion methods yielding $\beta_v^{\rm eff} > 2$, consistent with ASV [33], and as large as ≈ 2.6. However, with the double Mellin method the effective exponent is much closer to the NLO case, with $\beta_v^{\rm eff} \approx 1.2$ as $x \to 1$. This suggests that with currently available data and theoretical methods, we cannot distinguish between $\beta_v^{\rm eff} \sim 1$ and ~ 2 asymptotic behaviors.

Large systematics of threshold resummation prescriptions!

JAM21: Momentum Fractions
[Barry et al., PRL 127, 232001 (2021)]

TABLE II. Momentum fractions of the pion carried by valence quarks, sea quarks and gluons at the input scale, $\mu^2 = m_c^2$, and at $\mu^2 = 10$ GeV^2, for various combinations of data sets used in this analysis. The results for the full analysis ("DY+LN+DYp_T") are given in boldface.

	$\mu^2 = m_c^2$			$\mu^2 = 10$ GeV^2		
data sets	$\langle x\rangle_v^\pi$	$\langle x\rangle_s^\pi$	$\langle x\rangle_g^\pi$	$\langle x\rangle_v^\pi$	$\langle x\rangle_s^\pi$	$\langle x\rangle_g^\pi$
DY	0.59(1)	0.28(10)	0.13(11)	0.49(1)	0.26(8)	0.25(8)
DY+LN	0.53(2)	0.14(4)	0.34(6)	0.43(2)	0.17(3)	0.40(4)
DY+LN+DYp_T	**0.54(2)**	**0.16(3)**	**0.29(5)**	**0.44(1)**	**0.19(2)**	**0.37(3)**

TABLE I. Total momentum fractions of the valence quark, sea quark, and gluon distributions at the input scale $\mu = \mu_0$ for various resummation prescriptions.

resummation method	$\langle x\rangle_v$	$\langle x\rangle_s$	$\langle x\rangle_g$
NLO	0.53(2)	0.14(4)	0.34(6)
NLO+NLL cosine	0.47(2)	0.14(5)	0.39(6)
NLO+NLL expansion	0.46(2)	0.16(5)	0.38(6)
NLO+NLL double Mellin	0.46(3)	0.15(7)	0.40(5)

the double Mellin resummation favors a larger gluon at higher x

Pion PDFs

$$Q^2 = 9.6\ \mathrm{GeV}^2$$

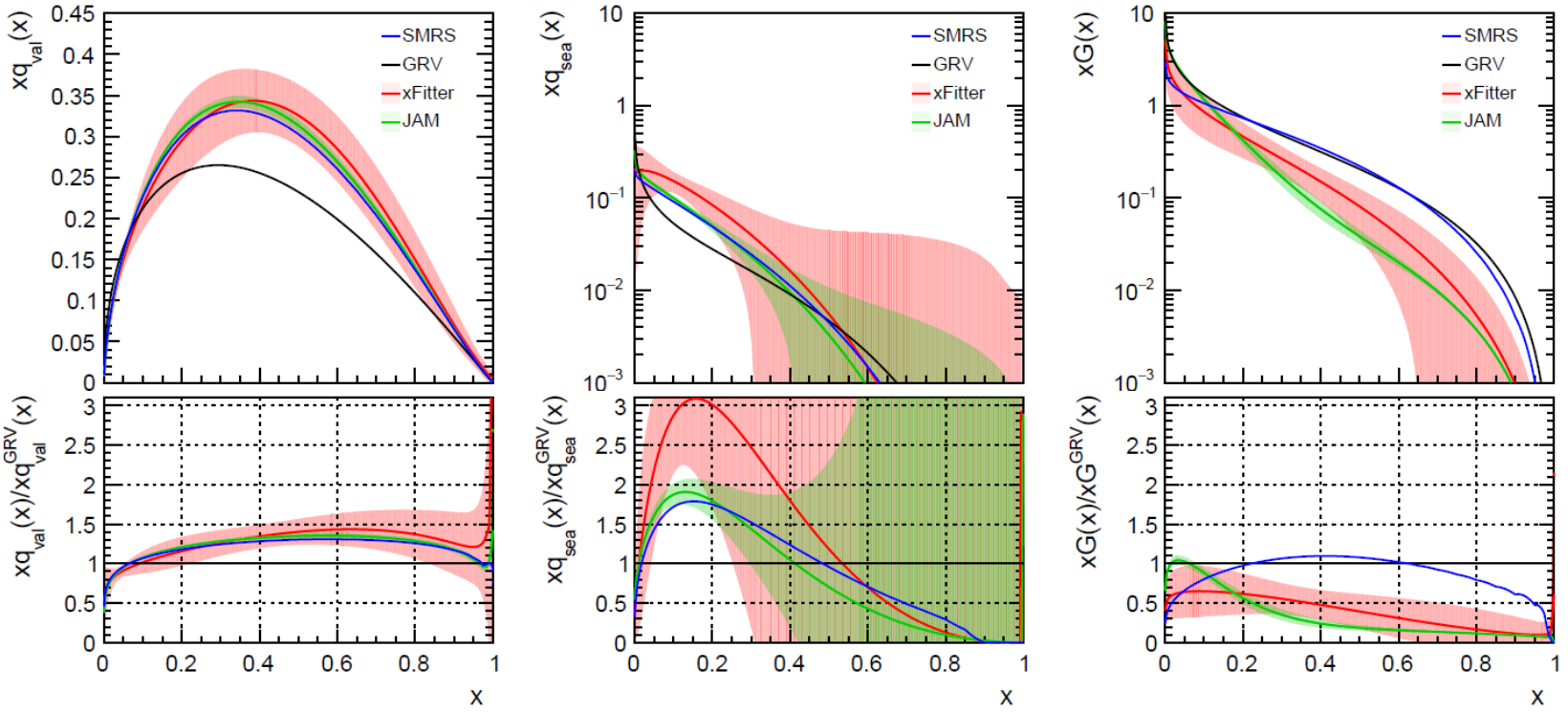

The gluon distributions of SMRS and GRV are significantly larger than JAM and xFitter for x>0.1.

Pion-induced J/psi Production - Fixed-target Experiments

Paper	Reference	Year	Collab	E (GeV)	sqrt(s) (GeV)	Beam	Targets
Fermilab							
Branson	PRL 23, 1331	1977	Princ-Chicago	225	20.5	π-, π+, p	C, Sn
Anderson	PRL 42, 944	1979	E444	225	20.5	π-, π+, K+, p, ap	C, Cu, W
Abramov	Fermi 91-062-E	1991	E672/E706	530	31.5	π-	Be
Kartik	PRD 41, 1	1990	E672	530	31.5	π-	C, AL, Cu, Pb
Katsanevas	PRL 60, 2121	1988	E537	125	15.3	π-, ap	Be, Cu, W
Akerlof	PR D48, 5067	1993	E537	125	15.3	π-, ap	Be, Cu, W
Antoniazzi	PRD 46, 4828	1992	E705	300	23.7	π-, π+	Li
Gribushin	PR D53, 4723	1995	E672/E706	515	31.1	π-	Be
Koreshev	PRL 77, 4294	1996	E706/E672	515	31.1	π-	Be
CERN							
Abolins	PLB 82, 145	1979	WA11/Goliath	150	16.8	π-	Be
McEwen	PLB 121, 198	1983	WA11	190	18.9	π-	Be
Badier	Z.Phys. C20, 101	1983	NA3	150	16.8	π-, π+, K-, K+, p, ap	H, Pt
"	"	1983	NA3	200	19.4	π-, π+, K-, K+, p, ap	H, Pt
"	"	1983	NA3	280	22.9	π-, π+, K-, K+, p, ap	H, Pt
Corden	PLB 68, 96	1977	WA39	39.5	8.6	π-, π+, K-, K+, p, ap	Cu
Corden	PLB 96, 411	1980	WA39	39.5	8.6	π-, π+, K-, K+, p, ap	W
Corden	PLB 98, 220	1981	WA39	39.5	8.6	π-, π+, K-, K+, p, ap	p
Corden	PLB 110, 415	1982	WA40	39.5	8.6	π-, π+, K-, K+, p, ap	p, W
Alexandrov	NPB 557, 3	1999	Beatrice	350	25.6	π-	Si, C, W

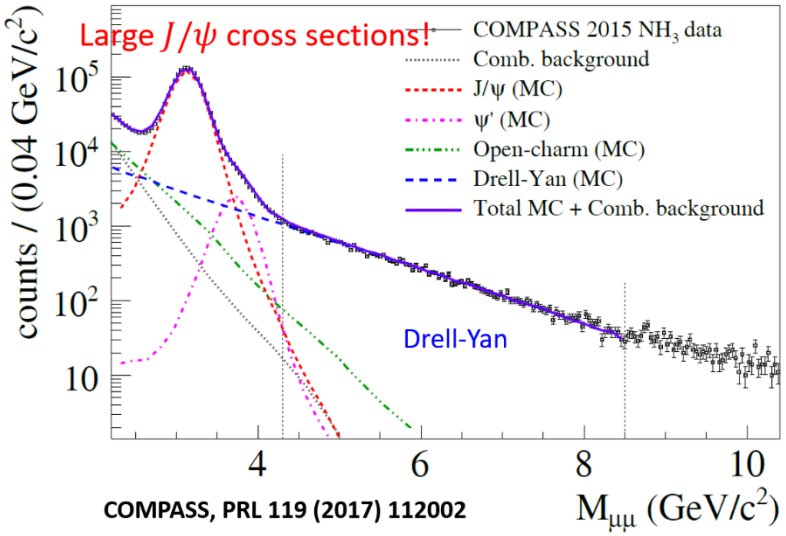

COMPASS, PRL 119 (2017) 112002

LO & NLO Diagrams of $c\bar{c}$ Production

LO

A. Petrelli et al./Nuclear Physics B 514 (1998) 245–309

$q\bar{q}$

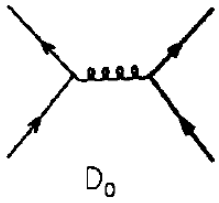

GG

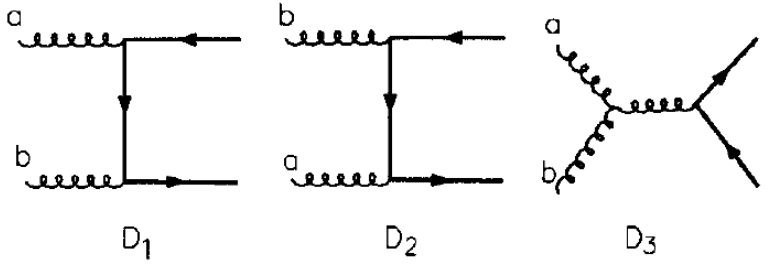

Fig. 2. Diagrams for the $q\bar{q}$ and g

NLO

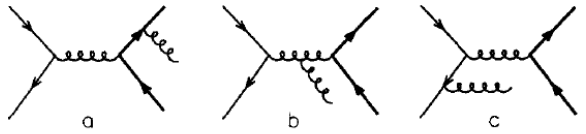

Fig. 8. Diagrams for the real corrections to the $q\bar{q}$ channels. Permutations of outgoing gluons and/or reversal of fermion lines are always implied.

qG

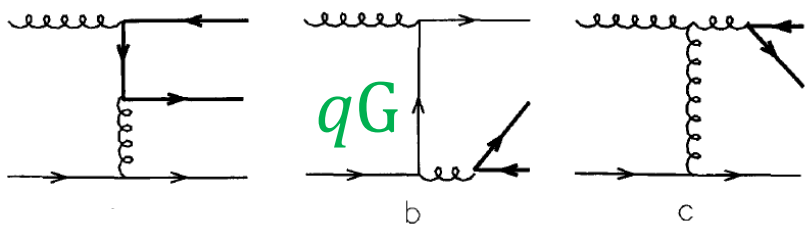

the gq channels. Reversal of fermion lines is always implied.

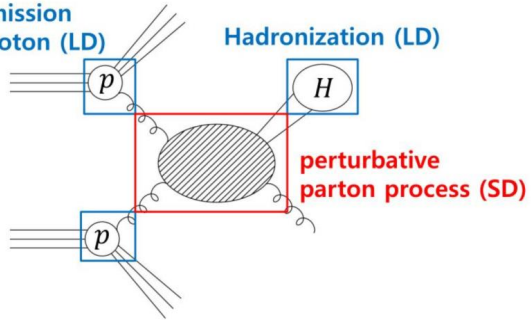

Model Dependence of $c\bar{c}$ Hadronization

- **Color singlet model (CSM)**: only pairs with matched quantum number of the charmonium.
- **Color evaporation model (CEM)**: all pairs with mass less than $D\bar{D}$ threshold. One hadronization parameter for each charmonium.
- **Non-relativistic QCD model (NRQCD)**: all pairs of different color and spin sates fragmenting with different probabilities – long-distance matrix elements (LDMEs).

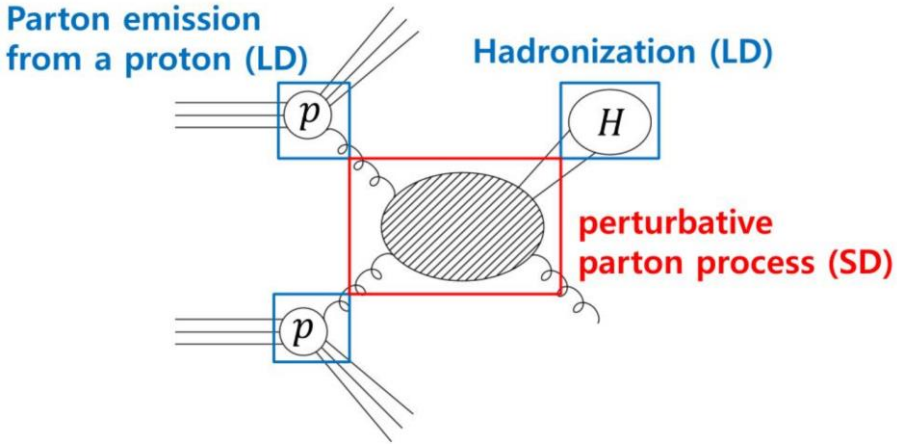

Color evaporation model (CEM)

Phys. Rev. D 102, 054024 (2020); arXiv: 2006.06947

PHYSICAL REVIEW D **102,** 054024 (2020)

Constraining gluon density of pions at large x by pion-induced J/ψ production

Wen-Chen Chang
Institute of Physics, Academia Sinica, Taipei 11529, Taiwan

Jen-Chieh Peng
Department of Physics, University of Illinois at Urbana-Champaign, Urbana, Illinois 61801, USA

Stephane Platchkov
IRFU, CEA, Université Paris-Saclay, 91191 Gif-sur-Yvette, France

Takahiro Sawada
Department of Physics, Osaka City University, Osaka 558-8585, Japan

(Received 12 June 2020; accepted 8 September 2020; published 24 September 2020)

The gluon distributions of the pion obtained from various global fits exhibit large variations among them. Within the framework of the color evaporation model, we show that the existing pion-induced J/ψ

Data vs. CEM NLO: $\sigma(\sqrt{s})$

$$\pi^- + N \rightarrow Jpsi + X$$

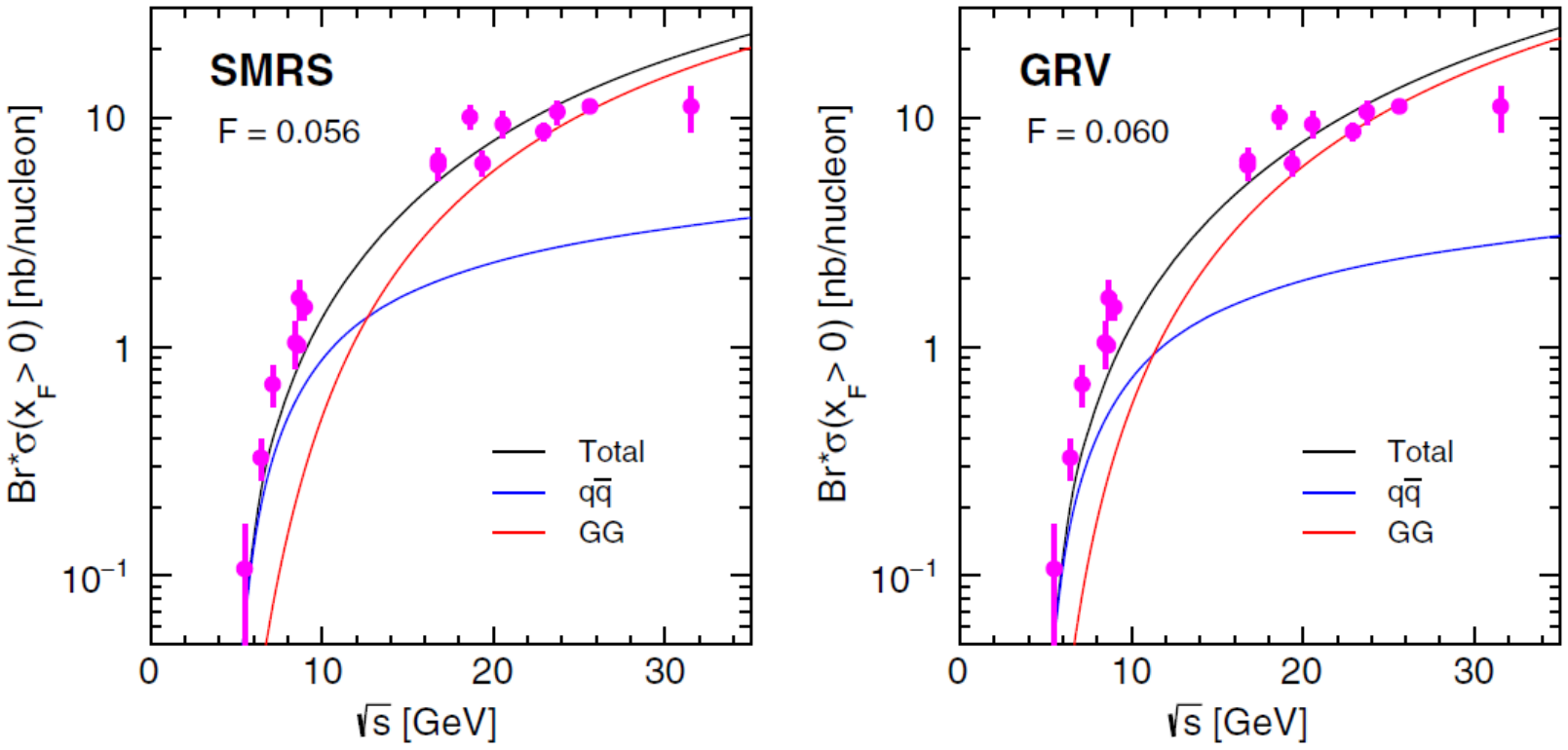

GG dominates at high energies, while $q\bar{q}$ is important near threshold.

Data vs. CEM NLO: $\sigma(\sqrt{s})$

$$\pi^- + N \rightarrow Jpsi + X$$

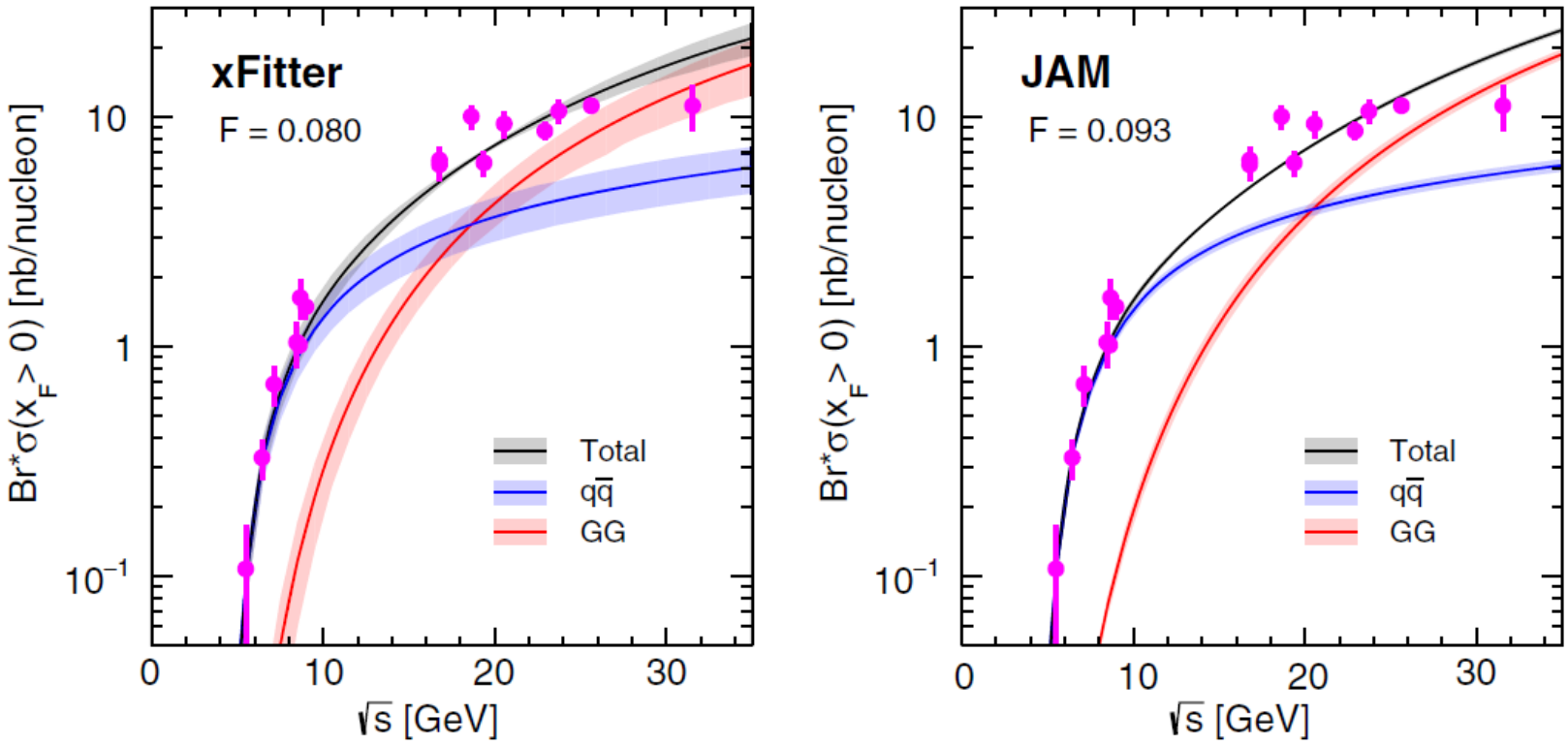

GG dominates at high energies, while $q\bar{q}$ is important near threshold.

Data vs. CEM NLO

[$\pi^- + Pt \rightarrow Jpsi + X$ at 200 GeV, Z. Phys. C20,101(1983)]

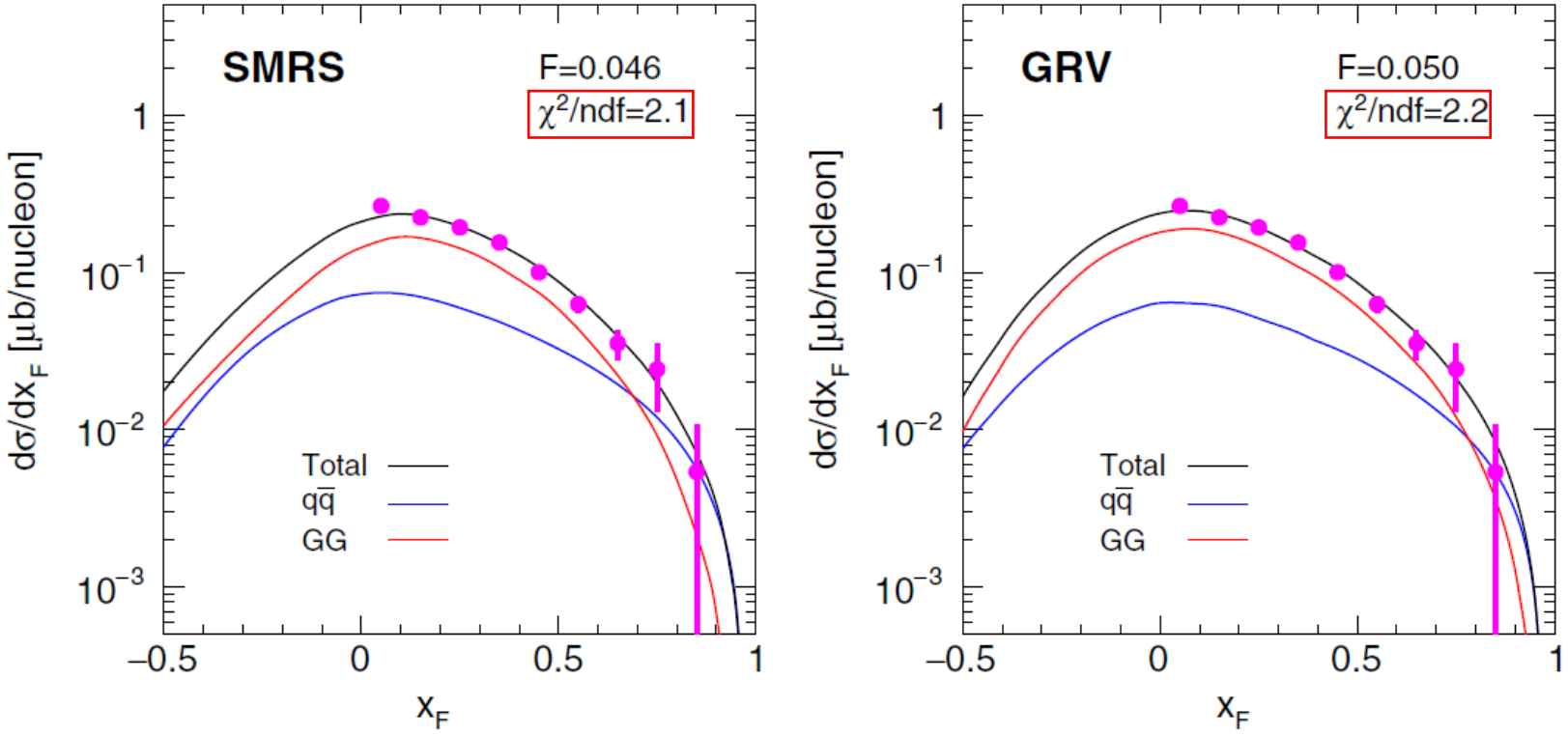

- The GG contribution dominates except at very forward or backward directions.
- To well describe the data for xF>0.2, an appropriate weighting of GG and $q\bar{q}$ contributions is necessary.

Data vs. CEM NLO

[$\pi^- + Pt \rightarrow Jpsi + X$ at 200 GeV, Z. Phys. C20,101(1983)]

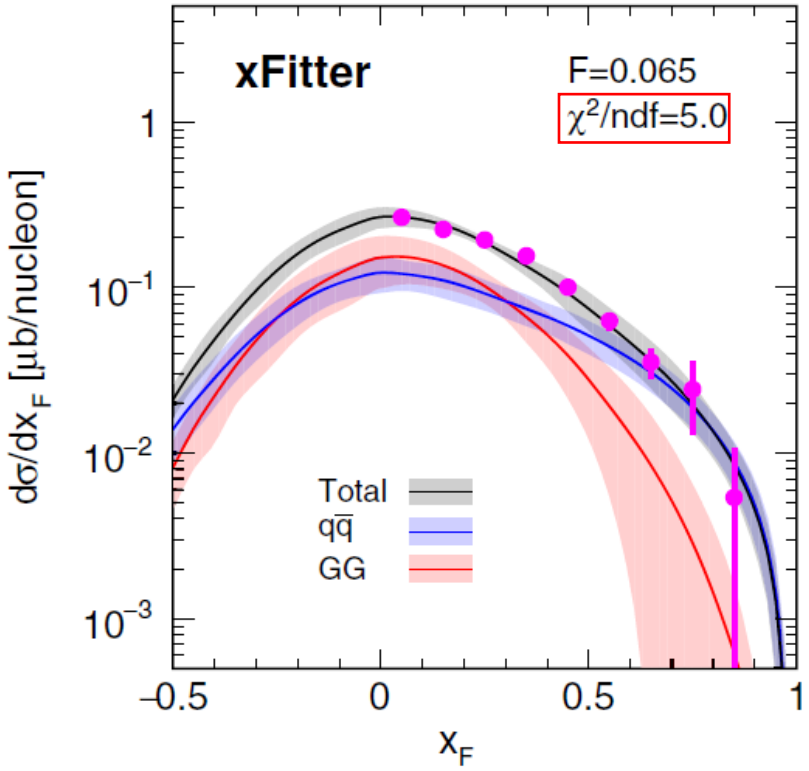

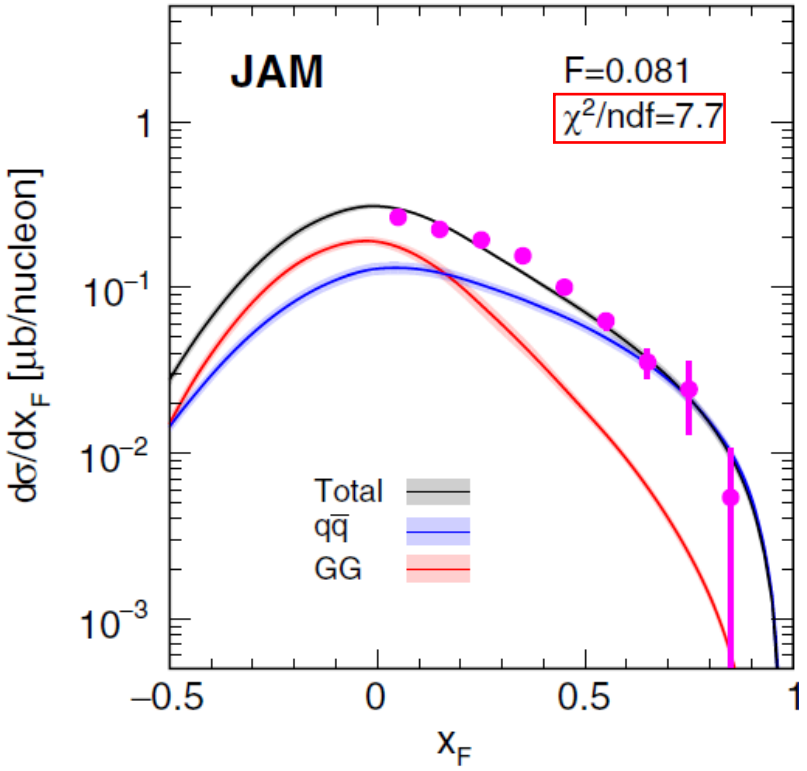

- The GG contribution dominates except at very forward or backward directions.
- To well describe the data for xF>0.2, an appropriate weighting of GG and $q\bar{q}$ contributions is necessary.

Data vs. CEM Calculations

TABLE III. Results of F factor and χ^2/ndf value of the best fit of the NLO CEM calculations for SMRS, GRV, xFitter, and JAM pion PDFs to the data listed in Table II. The F^* factor and χ^2/ndf^* are the ones corresponding to the fit with inclusion of PDF uncertainties for xFitter and JAM.

Data	SMRS		GRV		xFitter				JAM			
Experiment (P_{beam})	F	χ^2/ndf	F	χ^2/ndf	F	F^*	χ^2/ndf	χ^2/ndf*	F	F^*	χ^2/ndf	χ^2/ndf*
E672, E706 (515)	0.040	1.2	0.040	2.2	0.063	0.063	6.8	4.7	0.081	0.081	18.9	18.5
E705 (300)	0.052	2.3	0.053	1.9	0.073	0.076	3.2	1.3	0.086	0.086	16.1	15.9
NA3 (280)	0.046	1.5	0.049	2.0	0.067	0.069	5.0	3.2	0.081	0.081	10.4	10.3
NA3 (200)	0.046	2.1	0.050	2.2	0.065	0.066	5.0	1.3	0.081	0.081	7.7	7.6
WA11 (190)	0.054	5.0	0.058	7.2	0.078	0.076	19.4	6.2	0.091	0.091	73.7	72.9
NA3 (150)	0.065	1.1	0.071	1.0	0.089	0.091	2.6	1.6	0.108	0.108	3.9	3.8
E537 (125)	0.044	1.5	0.049	1.5	0.065	0.065	3.1	1.4	0.083	0.083	3.5	3.5
WA39 (39.5)	0.068	1.3	0.079	1.4	0.073	0.072	1.1	0.8	0.080	0.080	1.2	1.2

- The hadronization F factor is stable across energy.
- High-energy J/ψ data have a large sensitivity to the large-x gluon density of pions.
- The valence-quark distributions plays a minor role if away from the threshold.
- **CEM NLO calculations favor SMRS and GRV PDFs whose gluon densities at x > 0.1 are higher, compared with xFitter and JAM PDFs.**

Are these observations model dependent?

psi'/Jpsi(x_F)

Eur. Phys. J. C 49, 545–558 (2007)

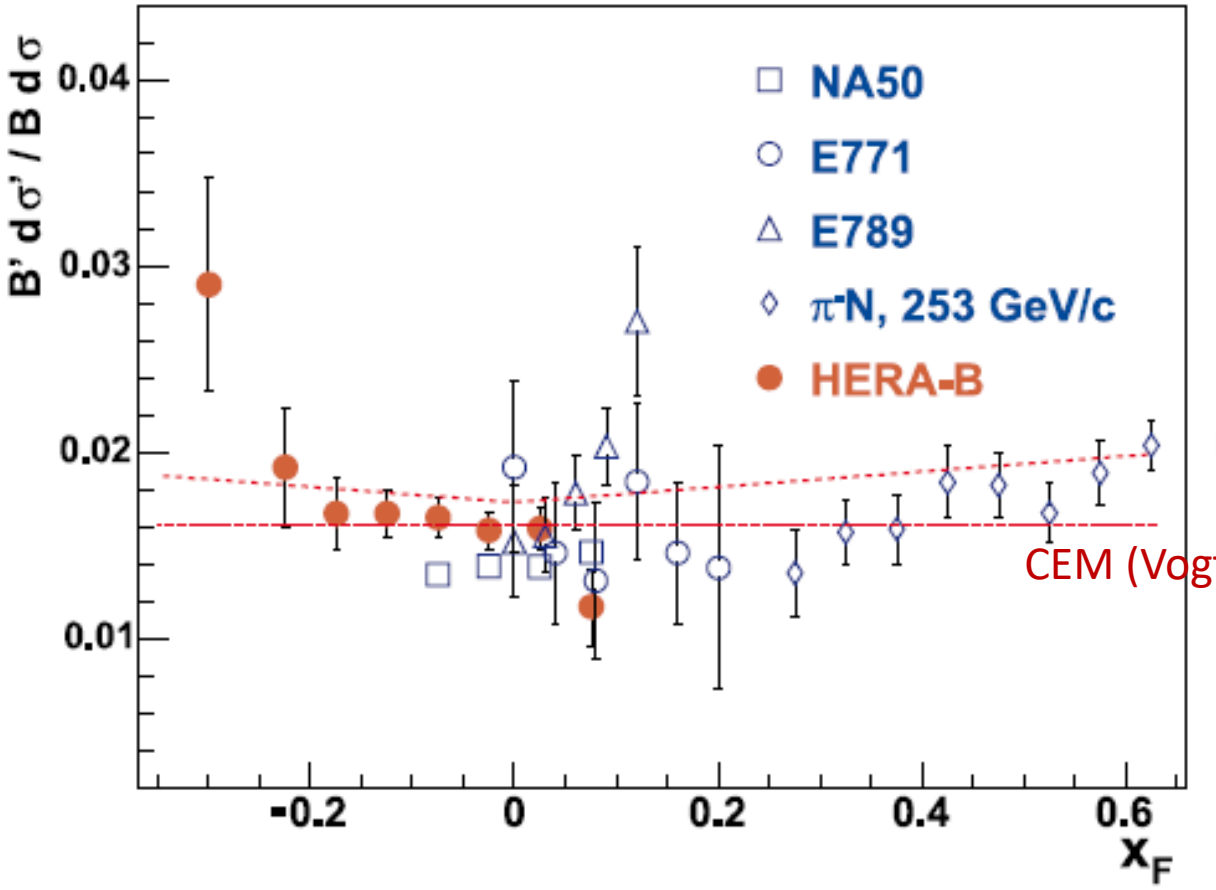

NRQCD (Vogt)

CEM (Vogt), flat over xF.

Naïve CEM calculation fails to describe the xF dependence of psi'/Jpsi.

Non-relativistic QCD model (NRQCD)

Chin.J.Phys. 73 (2021) 13; arXiv: 2103.11660

Contents lists available at ScienceDirect

Chinese Journal of Physics

journal homepage: www.elsevier.com/locate/cjph

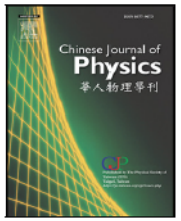

Check for updates

NRQCD analysis of charmonium production with pion and proton beams at fixed-target energies

Chia-Yu Hsieh [a,b,1], Yu-Shiang Lian [a,c,1], Wen-Chen Chang [a,*], Jen-Chieh Peng [d], Stephane Platchkov [e], Takahiro Sawada [f]

[a] Institute of Physics, Academia Sinica, Taipei 11529, Taiwan
[b] Department of Physics, National Central University, 300 Jhongda Road, Jhongli 32001, Taiwan
[c] Department of Physics, National Kaohsiung Normal University, Kaohsiung County 824, Taiwan
[d] Department of Physics, University of Illinois at Urbana-Champaign, Urbana, Illinois 61801, USA
[e] IRFU, CEA, Université Paris-Saclay, 91191 Gif-sur-Yvette, France
[f] Department of Physics, Osaka City University, Osaka 558-8585, Japan

ARTICLE INFO

Keywords:
Charmonium production
Pion PDFs
NRQCD
Color-octet matrix elements
Gluon

ABSTRACT

We present an analysis of hadroproduction of J/ψ and $\psi(2S)$ at fixed-target energies in the framework of non-relativistic QCD (NRQCD). Using both pion- and proton-induced data, a new determination of the color-octet long-distance matrix elements (LDMEs) is obtained. Compared with previous results, the contributions from the $q\bar{q}$ and color-octet processes are significantly enhanced, especially at lower energies. A good agreement between the pion-induced J/ψ production data and NRQCD calculations using the newly obtained LDMEs is achieved. We find that the pion-induced charmonium production data are sensitive to the gluon density of pions, and favor pion PDFs with relatively large gluon contents at large x.

(LO) NRQCD Framework
PRD 54, 2005 (1996)

PHYSICAL REVIEW D VOLUME 54, NUMBER 3 1 AUGUST 1996

Hadroproduction of quarkonium in fixed-target experiments

M. Beneke
Stanford Linear Accelerator Center, Stanford University, Stanford, California 94309

I. Z. Rothstein
University of California, San Diego, 9500 Gilman Drive, La Jolla, California 92093
(Received 25 March 1996)

We analyze charmonium and bottomonium production at fixed-target experiments. We find that the inclusion of color octet production channels removes large discrepancies between experiment and the predictions of the color singlet model for the total production cross section. Furthermore, including octet contributions accounts for the observed direct to total J/ψ production ratio. As found earlier for photoproduction of quarkonia, a fit to fixed-target data requires smaller color octet matrix elements than those extracted from high-p_t production at the Fermilab Tevatron. We argue that this difference can be explained by systematic differences in the velocity expansion for collider and fixed-target predictions. While the color octet mechanism thus appears to be an essential part of a satisfactory description of fixed-target data, important discrepancies remain for the χ_{c1}/χ_{c2} production ratio and J/ψ (ψ') polarization. These discrepancies, as well as the differences between pion- and proton-induced collisions, emphasize the need for including higher twist effects in addition to the color octet mechanism. [S0556-2821(96)05515-4]

PACS number(s): 13.85.Ni, 13.88.+e, 14.40.Gx

Long-Distance Matrix Elements (LDMEs) PRD 54, 2005 (1996)

$\left\langle O_{1,8}^{H}\left[{}^{2S+1}L_J\right]\right\rangle$

	$J/\psi,\ \psi(2S)$	χ_{c0}	χ_{c1}	χ_{c2}
$q\bar{q}$	$\langle \mathcal{O}_8^H[^3S_1]\rangle$	$\langle \mathcal{O}_8^H[^3S_1]\rangle$	$\langle \mathcal{O}_8^H[^3S_1]\rangle$	$\langle \mathcal{O}_8^H[^3S_1]\rangle$
GG	$\langle \mathcal{O}_1^H[^3S_1]\rangle$ $\Delta_8{}^*$	$\langle \mathcal{O}_1^H[^3P_0]\rangle$	$\langle \mathcal{O}_1^H[^3P_1]\rangle$	$\langle \mathcal{O}_1^H[^3P_2]\rangle$
qG			$\langle \mathcal{O}_1^H[^3P_1]\rangle$	

$$\Delta_8 = \langle \mathcal{O}_8^H[^1S_0]\rangle + \frac{3}{m_c^2}\langle \mathcal{O}_8^H[^3P_0]\rangle + \frac{4}{5m_c^2}\langle \mathcal{O}_8^H[^3P_2]\rangle$$

H	$\langle \mathcal{O}_1^H[^3S_1]\rangle$	$\langle \mathcal{O}_1^H[^3P_0]\rangle/m_c{}^2$	$\langle \mathcal{O}_8^H[^3S_1]\rangle$	$\langle \mathcal{O}_8^H[^1S_0]\rangle = \langle \mathcal{O}_8^H[^3P_0]\rangle/m_c{}^2$
J/ψ	1.16		6.6×10^{-3}	3.75×10^{-3}
$\psi(2S)$	0.76		4.6×10^{-3}	0.65×10^{-3}
χ_{c0}		0.044	3.2×10^{-3}	

Determined by fit of proton- and pion-indcued data

color-singlet (CS) LDMEs

color-octet (CO) LDMEs

$$\sigma_{J/\psi} = \sigma_{J/\psi}^{direct} + Br(\psi(2S)\to J/\psi X)\sigma_{\psi(2S)} + \sum_{J=0}^{2} Br(\chi_{cJ}\to J/\psi\gamma)\sigma_{\chi_{cJ}}$$

Jpsi & psi' Data vs. NRQCD

Best-fitted CO [3S1] and [1S0] LDMEs by p+N Jpsi/psi' and π^-+N Jpsi/psi' data.

J/Ψ

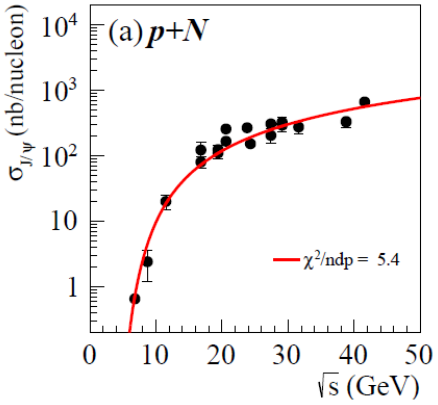

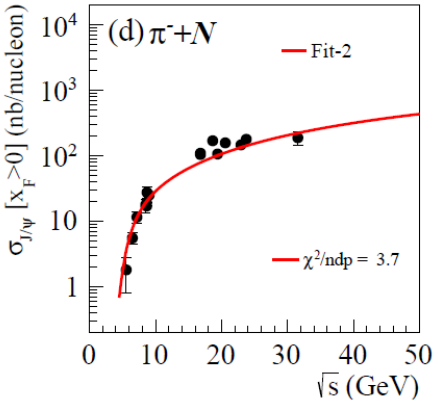

J/Ψ

Ψ'

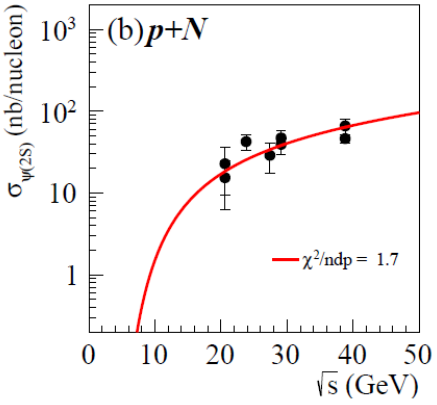

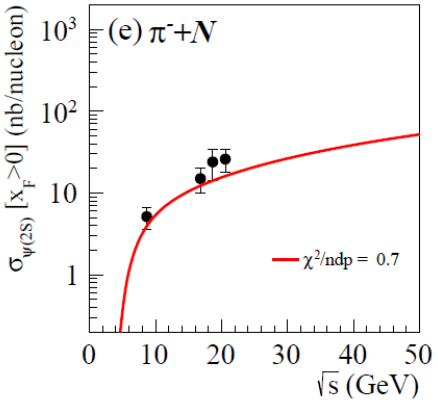

Ψ'

Proton PDFs: CT14nlo

Pion PDFs: GRV

$\langle \mathcal{O}_8^{J/\psi}[^3S_1] \rangle$	6.6×10^{-3}	$(1.47 \pm 0.07) \times 10^{-1}$	$(9.5 \pm 0.4) \times 10^{-2}$
$\langle \mathcal{O}_8^{J/\psi}[^1S_0] \rangle^*$	3.75×10^{-3}	$(0 \pm 1) \times 10^{-4}$	$(2.2 \pm 0.3) \times 10^{-3}$
$\langle \mathcal{O}_8^{\psi(2S)}[^3S_1] \rangle$	4.6×10^{-3}	$(2.5 \pm 0.2) \times 10^{-2}$	$(2.6 \pm 0.2) \times 10^{-2}$
$\langle \mathcal{O}_8^{\psi(2S)}[^1S_0] \rangle^*$	6.5×10^{-4}	$(0 \pm 1) \times 10^{-4}$	$(5 \pm 8) \times 10^{-5}$

π^-+N→Jpsi+X: pion PDFs

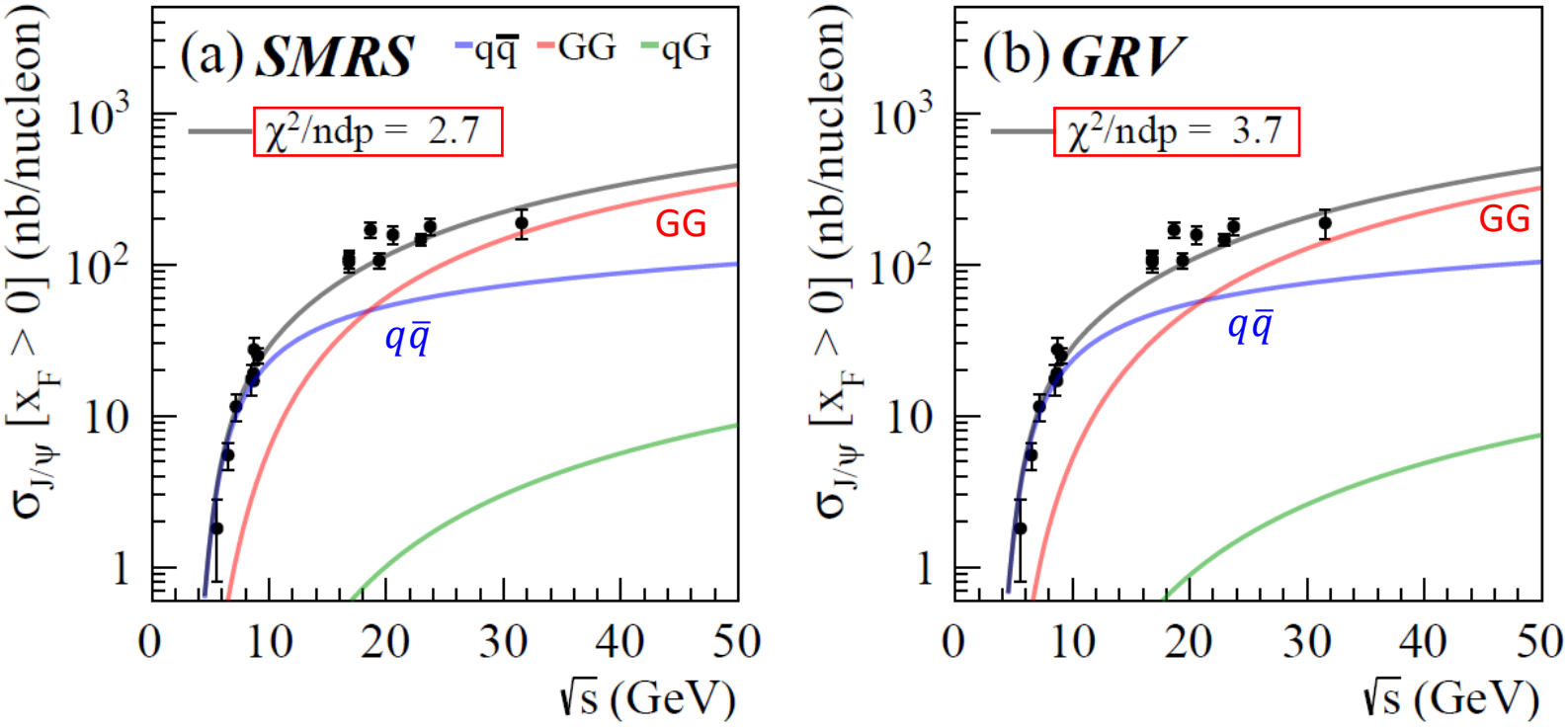

π^-+N→Jpsi+X: pion PDFs

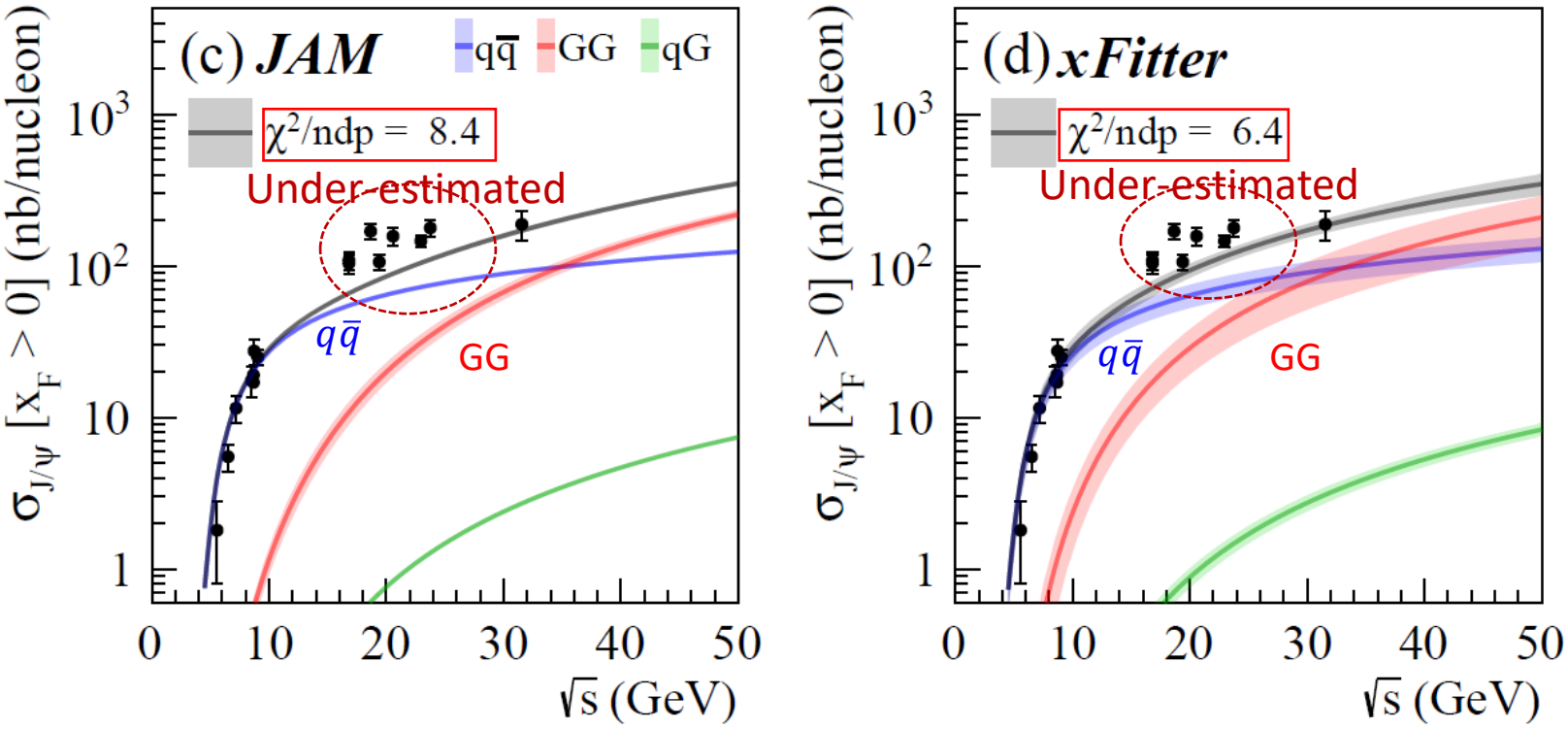

- The dependence of best-fit LDMEs to the pion PDFs is mild.
- The deficiency of JAM and xFitter in the GG contributions generates a relatively large χ^2 in the description of data.

Data of $d\sigma/dx_F$

Experiment	Beam	P_{beam} (GeV/c)	Target	Data	Normalization[a]	References
FNAL E672, E706	π	515	Be	$\sigma^{J/\psi}$	12.0	[59]
FNAL E705	π	300	Li	$\sigma^{J/\psi}$	9.5	[60]
CERN NA3[b]	π	280	p	$\sigma^{J/\psi}$	13.0	[61]
CERN NA3[b]	π	200	p	$\sigma^{J/\psi}$	13.0	[61]
CERN WA11[b]	π	190	Be	$\sigma^{J/\psi}$	[c]10.0	[62]
CERN NA3[b]	π	150	p	$\sigma^{J/\psi}$	13.0	[61]
FNAL E537	π	125	Be	$\sigma^{J/\psi}$	6.0	[63]
CERN WA39[b]	π	39.5	p	$\sigma^{J/\psi}$	15.0	[64]
FNAL E672, E706	π	515	Be	$\sigma^{\psi(2S)}$	16.0	[59]
FNAL E615	π	253	W	$\sigma^{\psi(2S)}/\sigma^{J/\psi}$		[74]
HERA-B	p	252	W	$\sigma^{\psi(2S)}/\sigma^{J/\psi}$		[75]
CERN NA50	p	450	W	$\sigma^{\psi(2S)}/\sigma^{J/\psi}$		[76]
FNAL E789	p	800	Au	$\sigma^{\psi(2S)}/\sigma^{J/\psi}$		[77]
FNAL E771	p	800	Si	$\sigma^{\psi(2S)}/\sigma^{J/\psi}$		[78]
FNAL E705	p	300	Li	$\sigma^{J/\psi}$	10.1	[60]
CERN NA3[b]	p	200	p	$\sigma^{J/\psi}$	[c]10.0	[61]

Data vs. NRQCD

- Global analysis of fixed-target charmonium production

$\sigma(\sqrt{s})$

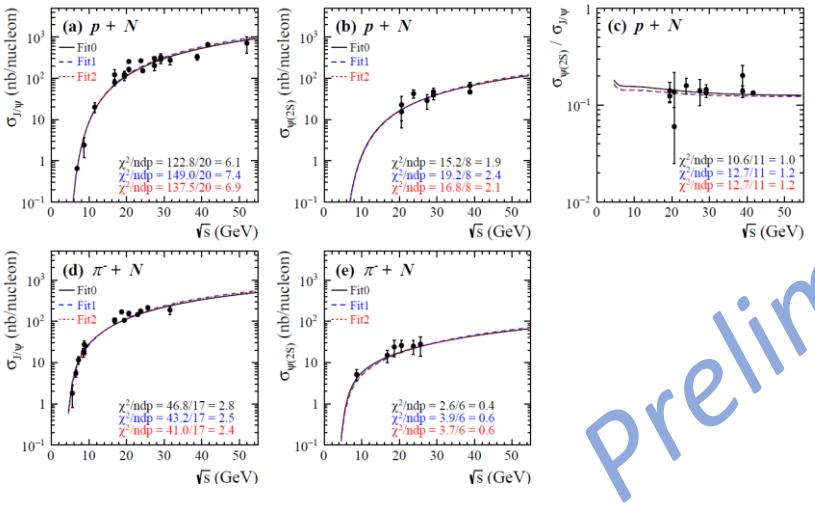

$\frac{d\sigma}{dx_F}$

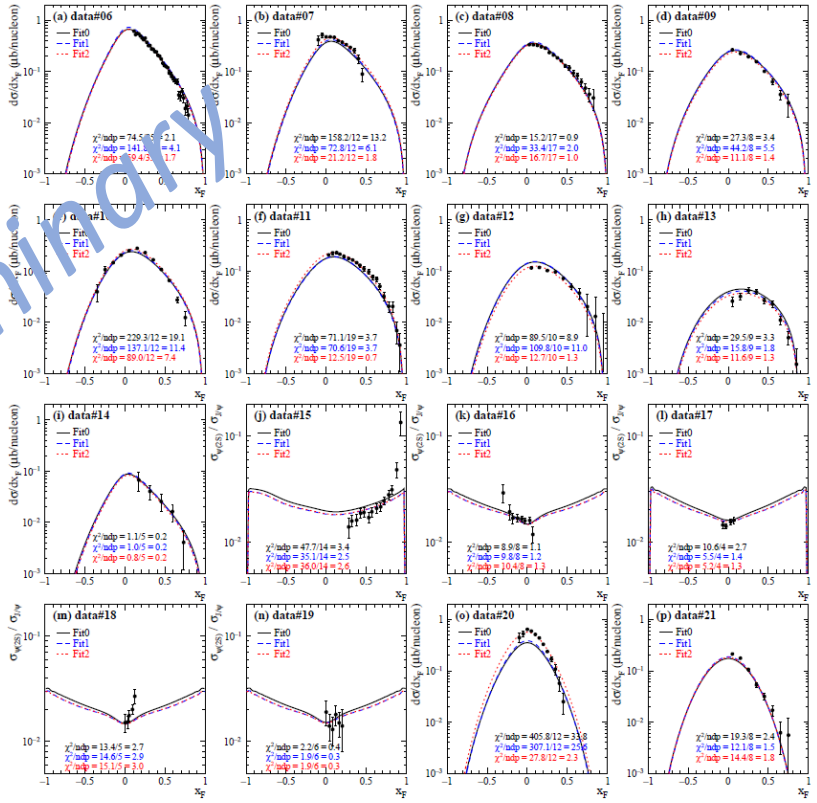

Preliminary

- Data
  - Jpsi, psi' and their ratios
  - Proton, pion beams
  - Integrated and differential x_F cross sections
- NRQCD calculations
  - Pion PDFs (SMRS, GRV, JAM and xFitter)
  - Proton PDFs (CT14nlo)
  - LDMEs

We can achieve a reasonable description of the charmonium data with the proton and pion beams by NRQCD calculations with similar LDMEs obtained in Chin. J. Phys. 73 (2021) 13.

Data vs. NRQCD

[$\pi^- + Pt \rightarrow Jpsi + X$ at 200 GeV, Z. Phys. C20,101(1983)]

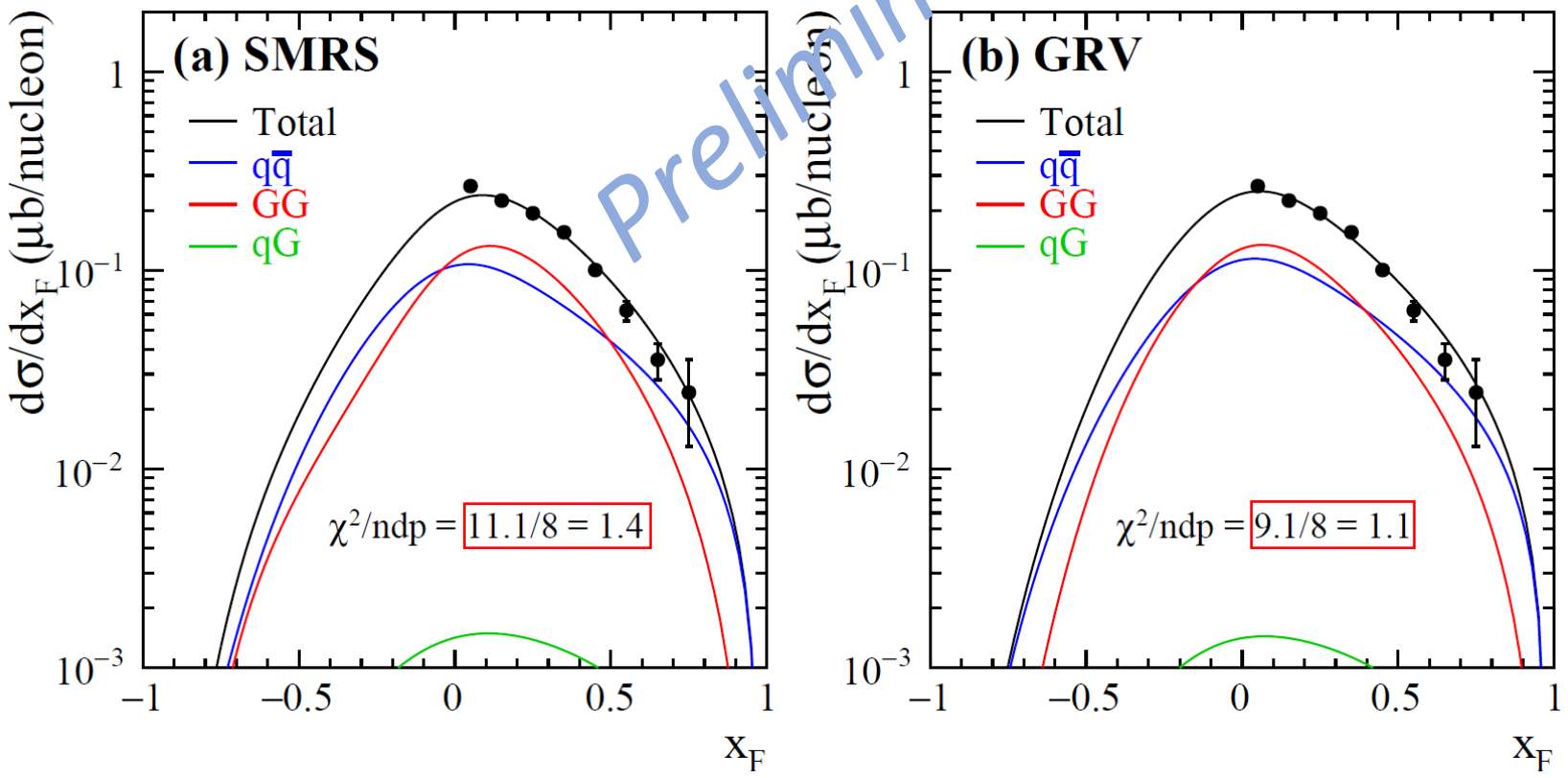

- The GG contribution dominates around xF=0.

Data vs. NRQCD

[$\pi^- + Pt \rightarrow Jpsi + X$ at 200 GeV, Z. Phys. C20,101(1983)]

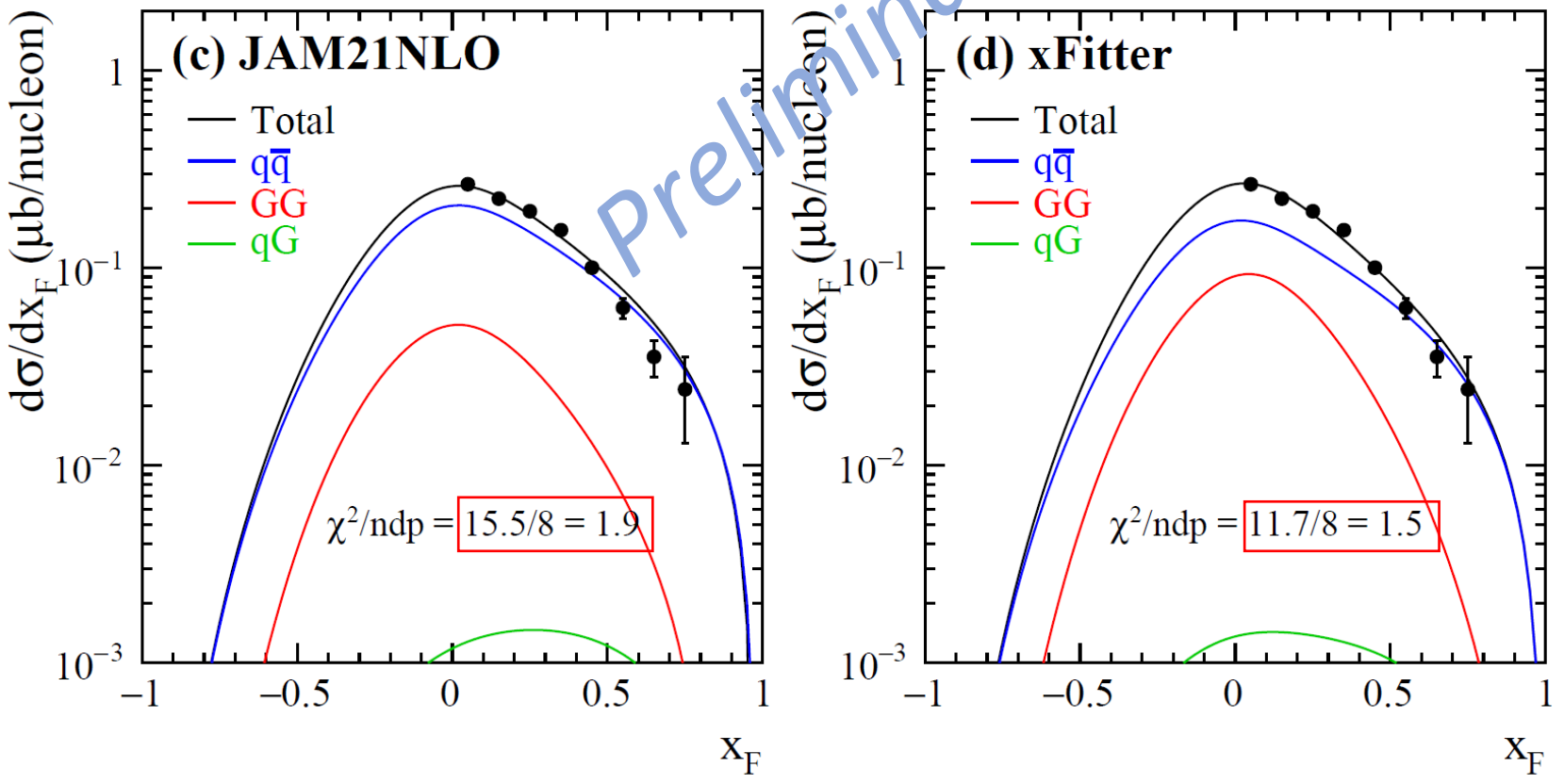

The $q\bar{q}$ contribution dominates the whole xF.

Data vs. NRQCD

[$\pi^- + Be \rightarrow Jpsi/psi' + X$ at 515 GeV, PRD 53, 4723 (1996)]

J/Ψ Ψ'

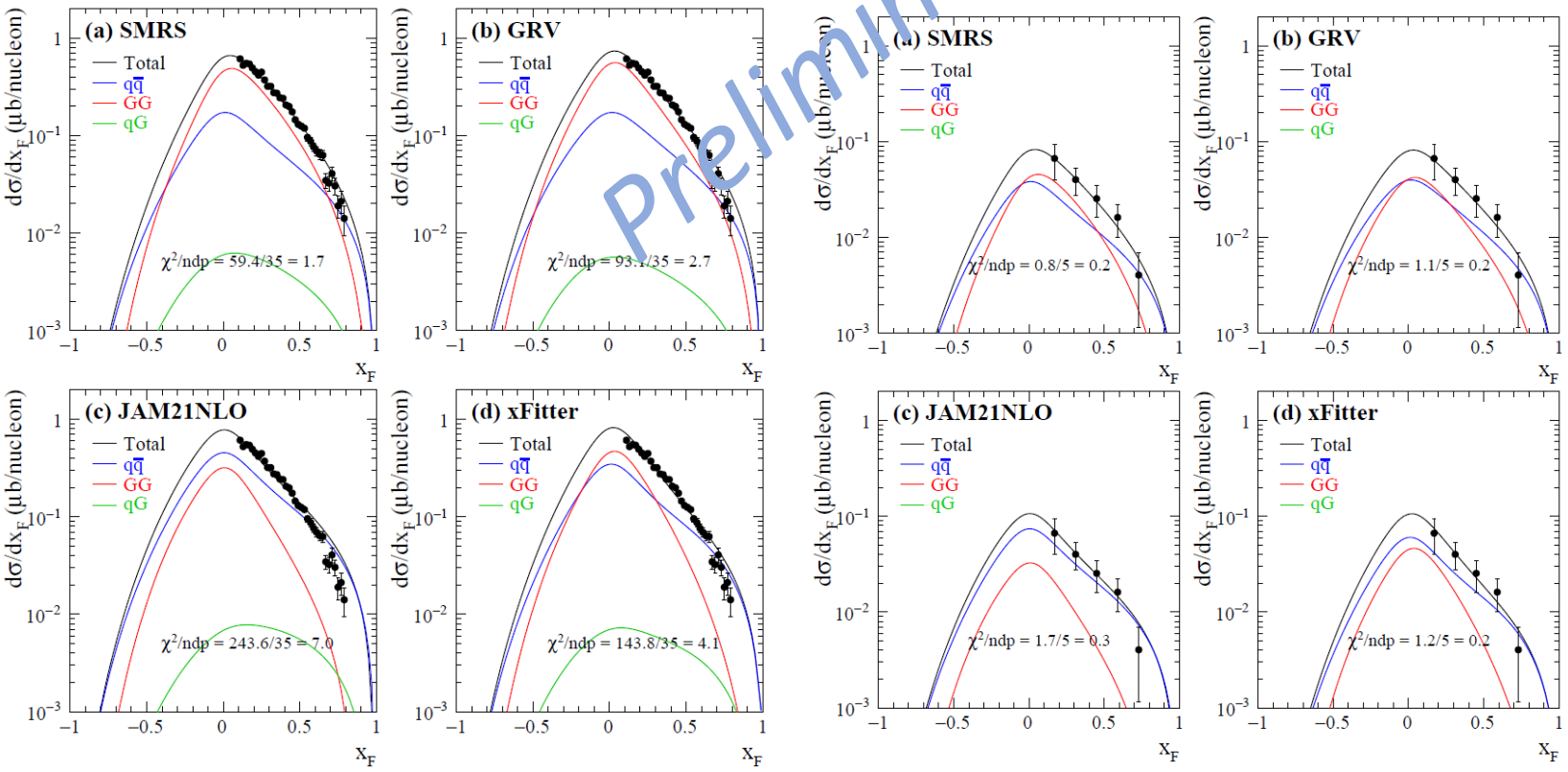

Relatively the $q\bar{q}$ process plays a more significant role in the production of Ψ', compared with J/Ψ .

psi'/Jpsi(xF)

[$\pi^- + W \rightarrow Jpsi/psi' + X$ at 253 GeV, PRD 53, 4723 (1996)]

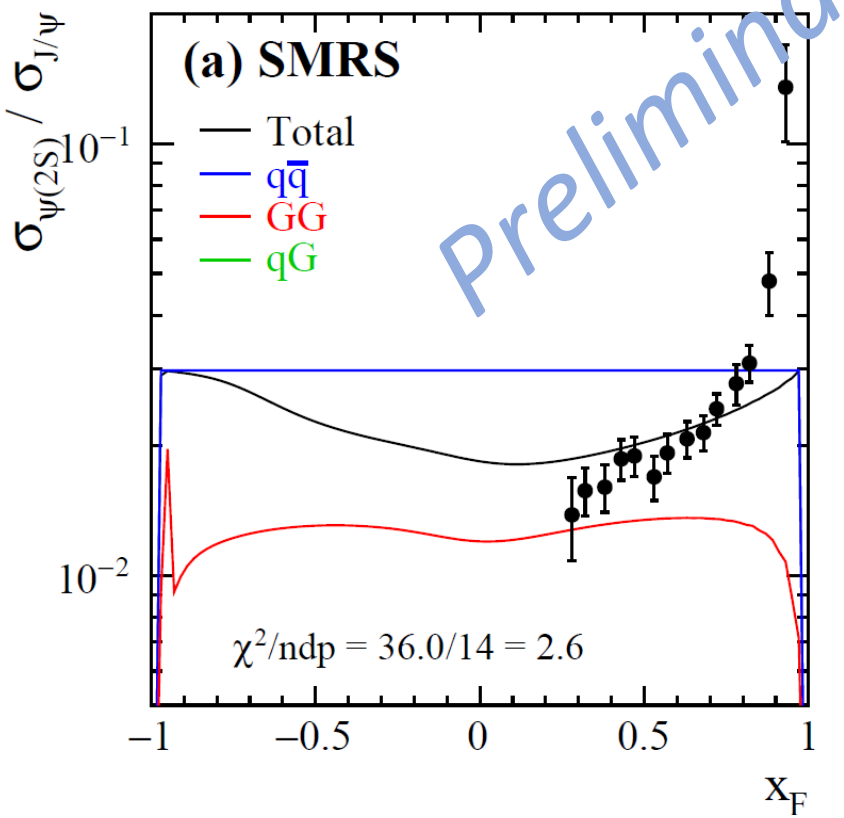

More discussions in Jen-Chieh's talk

The non-flat xF dependence of psi'/Jpsi can be accounted by NRQCD and could possibly be improved with inclusion of higher-order QCD effects.

Pion PDFs: DY + Jpsi

Phys.Rev.D 105 (2022) 076018 ; arXiv: 2202.12547

PHYSICAL REVIEW D **105,** 076018 (2022)

Pion partonic distributions in a statistical model from pion-induced Drell-Yan and J/Ψ production data

Claude Bourrely,[1] Wen-Chen Chang,[2] and Jen-Chieh Peng[3]

[1]*Aix Marseille Univ, Université de Toulon, CNRS, CPT, Marseille, France*
[2]*Institute of Physics, Academia Sinica, Taipei 11529, Taiwan*
[3]*Department of Physics, University of Illinois at Urbana-Champaign, Urbana, Illinois 61801, USA*

(Received 23 February 2022; accepted 6 April 2022; published 26 April 2022)

We present a new analysis to extract pion parton distribution functions (PDFs) within the framework of the statistical model. Starting from the statistical model first developed for the spin-1/2 nucleon, we extend this model to describe the spin-0 pion. Based on a combined fit to both the pion-induced Drell-Yan data and the pion-induced J/Ψ production data, a new set of pion PDFs has been obtained. The inclusion of the J/Ψ production data in the combined fit has provided additional constraints for better determining the gluon distribution in the pion. We also compare the pion PDFs obtained in the statistical model with other existing pion PDFs.

Statistical Model: DY + Jpsi

Phys.Rev.D 105 (2022) 076018 ; arXiv: 2202.12547

$$xU(x) = xD(x) = \frac{A_U X_U x^{b_U}}{\exp[(x - X_U)/\bar{x}] + 1} + \frac{\tilde{A}_U x^{\tilde{b}_U}}{\exp(x/\bar{x}) + 1}$$

$$x\bar{U}(x) = x\bar{D}(x) = \frac{A_U (X_U)^{-1} x^{b_U}}{\exp[(x + X_U)/\bar{x}] + 1} + \frac{\tilde{A}_U x^{\tilde{b}_U}}{\exp(x/\bar{x}) + 1}$$

$$xS(x) = x\bar{S}(x) = \frac{\tilde{A}_U x^{\tilde{b}_U}}{2[\exp(x/\bar{x}) + 1]}$$

$$xG(x) = \frac{A_G x^{b_G}}{\exp(x/\bar{x}) - 1}, \qquad b_G = 1 + \tilde{b}_U$$

J/Ψ WA39 and NA3 J/ψ (π^- H_2)

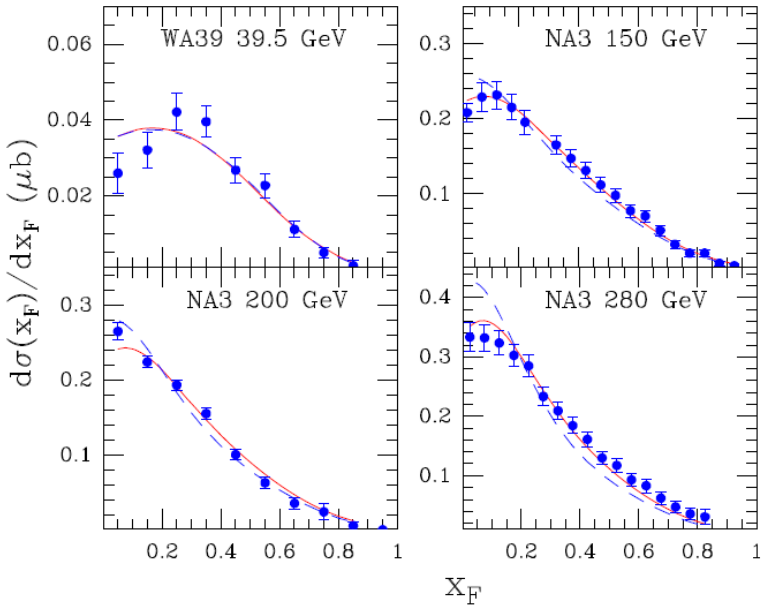

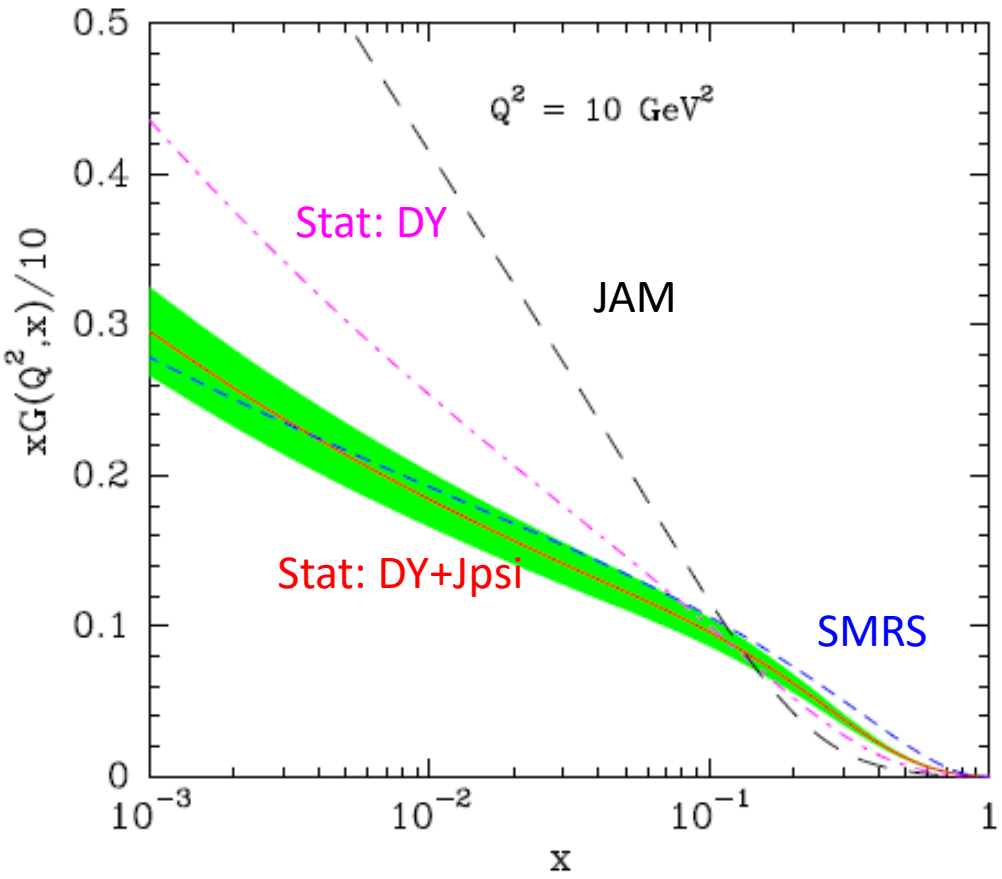

Constrains from Jpsi data:
xG(DY+Jpsi) > xG(DY) for x>0.1

Summary

- Significant discrepancy of valence quark and gluon densities at x>0.1 is seen among the pion PDFs.
- Within CEM and NRQCD, the high-energy J/psi data are shown to be sensitive to the pion gluon distribution. The current data favor the SMRS and GRV pion PDFs with relatively stronger gluon at large x.
- Within NRQCD, the psi' data is found to sensitive to the $q\bar{q}$ contribution, similar to DY.
- The pion(kaon)-induced charmonium data from COMPASS and AMBER shall provide good constrains on the large-x gluon distributions of pions (kaons).